

## Dissipation of Energy and Angular Momentum by Emission of Neutrons and Gamma Rays\*

J. ROBB GROVER

*Chemistry Department, Brookhaven National Laboratory, Upton, New York*

AND

JACOB GILAT†

*Chemistry Department, State University of New York at Stony Brook, Stony Brook, New York and  
Chemistry Department, Brookhaven National Laboratory, Upton, New York*

(Received 29 July 1966)

We examine quantitatively some of the consequences of the statistical theory of nuclear de-excitation for neutron and  $\gamma$ -ray emission from highly excited nuclei. Special attention is given to the dissipation of angular momentum. To a first approximation, the nuclear "thermal energy" is removed first, initially by neutron and then by dipole  $\gamma$ -ray emission. The "rotational energy" is dissipated afterwards as a cascade of low-energy  $\gamma$  rays which may be composed of a high proportion of quadrupole radiation. The meager experimental data available are consistent with the theoretical expectations, but do not as yet permit a crucial test. Further possible experiments are pointed out. The role of the lowest-energy excited state at every angular momentum (yrast levels) is taken into account explicitly. The importance of using correct level densities at energies near the yrast levels, where the conventional level-density formulas may be very inaccurate, is stressed.

### INTRODUCTION

WE see from the first paper of this series<sup>1</sup> that if one uses only the statistical-model "evaporation" theory to describe the de-excitation of a compound nucleus, and carries the calculation through without making the ruinous approximations that have had to be made in the past, many previously puzzling phenomena are reproduced. We obtain the high total  $\gamma$  energy, the low average  $\gamma$  energy, considerable quadrupole  $\gamma$  enhancement, essentially correct cross sections, and reasonable  $\gamma$  and particle spectra so far as these are known. We emphasize that to achieve these results we did not perform any parameter adjustment whatever; our input data were selected to be as relevant as possible to our sample system, in ignorance of what our calculation would subsequently show.

The explanation for many of our results is not necessarily obvious from the equations involved or the input data, but may become clear only after an enormous amount of bookkeeping has been performed by the computer. We have therefore tried to reduce the great mass of digital information provided by the computer to more qualitative and diagrammatic terms, in order to explain more easily why and how some of the interesting features described above arise.

The discussion of this paper is also intended to comprise background material for additional papers (e.g., Ref. 2).

\* Research performed in part under the auspices of the U. S. Atomic Energy Commission.

† Present address: Israel Atomic Energy Commission, Soreq Nuclear Research Center, Yavne, Israel.

<sup>1</sup> J. R. Grover and J. Gilat, preceding paper, Phys. Rev. **157**, 802 (1967).

<sup>2</sup> J. R. Grover and J. Gilat, first following paper, Phys. Rev. **157**, 823 (1967).

Our discussion is broken into three topics. First, we describe a special region of nuclear excitation energy and angular momentum in which  $\gamma$ -ray emission predominates although particle emission may be possible. For convenience, we call this region the " $\gamma$ -cascade band." Second, we describe the characteristics of  $\gamma$ -ray emission in terms of the  $\gamma$ -cascade band, and of details in the positioning of the yrast levels.<sup>3</sup> Third, we describe patterns in the distributions of population with respect to excitation energy and angular momentum in the nuclei involved, with special reference to the role played by the  $\gamma$ -cascade band.

### THE $\gamma$ -CASCADE BAND

As previously stressed,<sup>4</sup> the yrast levels play a crucial role in the de-excitation of excited nuclei of high angular momentum. We discuss this role in terms of several schematic diagrams, of which Fig. 1 is the

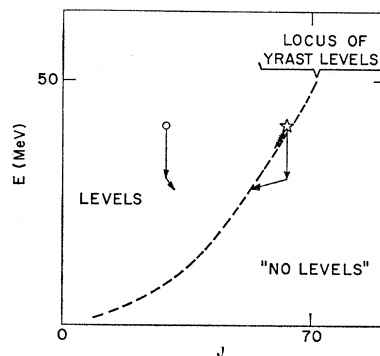
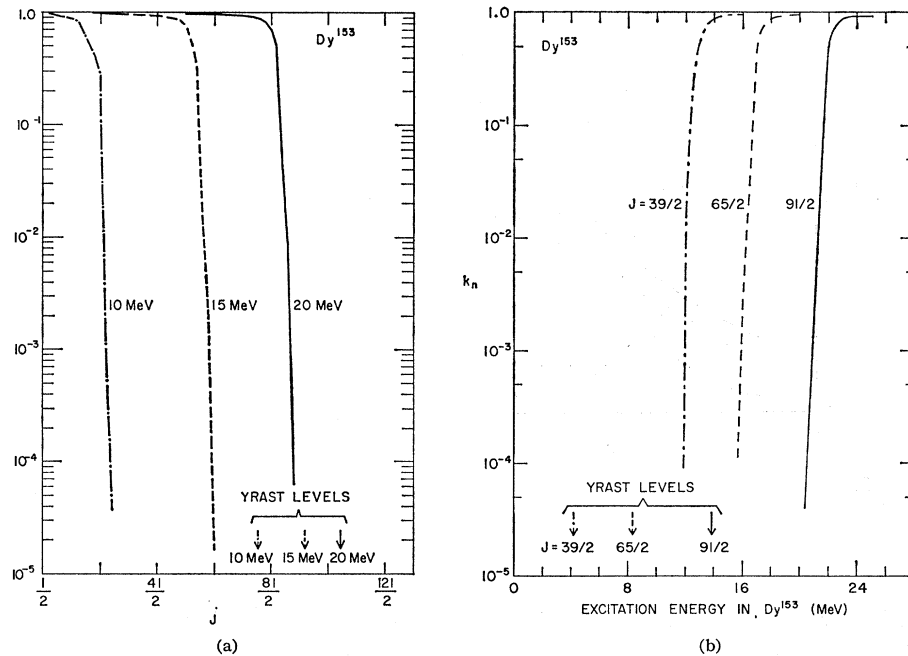


FIG. 1. Schematic diagram used to illustrate features of the de-excitation of highly excited nuclei with large angular momenta. Angular momentum is plotted on the abscissa and excitation energy on the ordinate (note that in the corresponding diagram in Ref. 4, the opposite choice of coordinates is used).

<sup>3</sup> J. R. Grover, second following paper Phys. Rev. **157**, 832 (1967).

<sup>4</sup> J. R. Grover, Phys. Rev. **127**, 2142 (1962).

FIG. 2. (a) Fraction  $k_n$  of  $\text{Dy}^{153}$  nuclei de-exciting by neutron emission, at excitation energies of  $E=10, 15,$  and  $20$  MeV, plotted as a function of angular momentum  $J$ . (b) Fraction  $k_n$  of  $\text{Dy}^{153}$  nuclei de-exciting by neutron emission, at angular momenta of  $39/2, 65/2,$  and  $91/2$ , plotted as a function of excitation energy.



first. Here, the abscissa represents the angular momentum of a nucleus, the ordinate the excitation energy; all the schematic diagrams have the same coordinates. For a given nucleus, the yrast levels can, for illustrative purposes, conveniently be represented as a line,<sup>3,4</sup> shown dashed in Fig. 1.

Consider the emission of a neutron from the nucleus at the excitation energy and angular momentum represented by the open circle. The neutron's binding energy is represented by a vertical solid arrow (pointing down for positive binding energy). To represent its kinetic properties we use a canted arrow joining the end of the vertical arrow. The horizontal displacement of the point of the kinetic arrow is intended to take account of the angular momentum removed by the outgoing neutron. (To keep the diagram simple we neglect the small intrinsic spin of the neutron, and, more serious, we use only one yrast line to represent both the neutron-emitting nucleus and the product nucleus.) Now the point of the kinetic arrow must not fall below the yrast line, for this is the region where the residual nucleus has "no levels."<sup>5</sup> For the excited nucleus represented by the open circle, however, there is still an ample region of the  $E$ - $J$  plane in which the kinetic arrow can terminate, and thus to which neutron emission can proceed. In this case neutron emission en-

counters no serious restraints and proceeds with a high rate. On the other hand, consider the emission of a neutron from the nucleus having the energy and angular momentum represented in the  $E$ - $J$  plane of Fig. 1 by the position of the open star. The binding-energy arrow terminates in the forbidden region below the yrast line. The kinetic arrow, which *must* terminate at or above the yrast line is thus forced to reach far to the left. This is just a way of showing that the outgoing neutron must carry away many units of angular momentum. To do so it must penetrate an angular-momentum barrier. The neutron-emission rate may thus be considerably smaller here than at the position represented by the open circle.

The total de-excitation rate of an excited nucleus always includes a contribution from  $\gamma$ -ray emission.<sup>6</sup> Since  $\gamma$  rays have neither a binding energy nor a Coulomb barrier, the first vertical arrow is omitted on a diagram such as Fig. 1, and we have only the "kinetic" arrow left to consider. Thus, as we draw sufficiently close to the yrast line where neutron emissions must penetrate formidable centrifugal potentials, the  $\gamma$  rays may still be emitted relatively freely, as indicated by the wavy arrow beginning at the star. Under these circumstances,  $\gamma$ -ray emission may well become the dominant mode of de-excitation, provided charged-particle emission is not important. That this is calculated to happen is shown in Figs. 2(a) and 2(b). Figure 2(a) is a plot of  $k_n$  versus  $J$  at constant excitation energies of 10, 15, and 20 MeV in  $\text{Dy}^{153}$ . Similarly, in

<sup>5</sup> In general, this region of the  $E$ -versus- $J$  diagram is in the continuum for a variety of two-body and more complicated states. For example, often, even the ground-state nucleus will have a positive  $Q$  for fission, alpha decay, etc. At higher excitation energies more such continuum states become possible. We assume here that the transitions to the three- (and more) body final states, implied by the termination of the kinetic arrow at energies less than those of the yrast levels, proceed with such slow rates that they may be neglected. See Ref. 3.

<sup>6</sup> An exception may be when only a monopole transition is possible. However, even here de-excitation may take place by internal conversion processes.

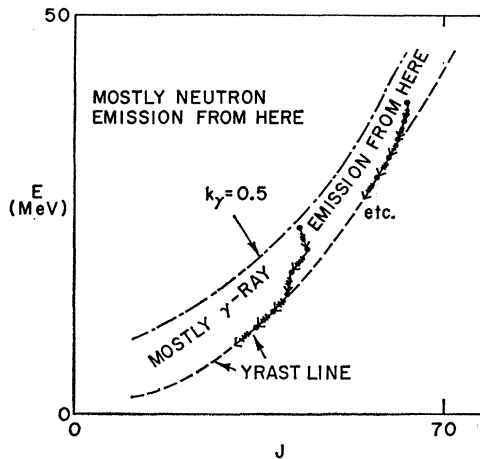


FIG. 3. Schematic diagram illustrating region of excitation energy and angular momentum in which most de-excitation is by  $\gamma$  radiation, i.e., the  $\gamma$ -cascade band. The symbol  $k_\gamma$  expresses the fraction of nuclei de-exciting by  $\gamma$ -ray emission.

Fig. 2(b) we plot  $k_n$  against excitation energy at constant  $J$  of  $39/2$ ,  $65/2$ , and  $91/2$  in the same nucleus. Here

$$k_n = \langle \Gamma_n \rangle / \langle \Gamma_{\text{total}} \rangle \approx \langle \Gamma_n / \Gamma_{\text{total}} \rangle,$$

where  $\langle \Gamma_n(E, J) \rangle$  is the mean width for neutron emission of levels in  $\text{Dy}^{153}$  near excitation energy  $E$  and spin  $J$ , while  $\langle \Gamma_{\text{total}}(E, J) \rangle$  is the corresponding mean width for all de-excitation processes. Of special interest is the very steep drop of the relative neutron-emission probability  $k_n$  at values of  $J$  considerably below (or excitation energies considerably above) the corresponding yrast levels. Once  $k_n$  has dropped below 0.5, at any given  $J$ ,  $\gamma$ -ray emission takes over almost completely within a few tenths of a MeV<sup>7</sup> and becomes the main de-exciting process.

Just as we represented the yrast levels as a line on Fig. 1, we may indicate by a line that locus of energy versus spin for which  $k_\gamma = 0.5$ , i.e., the line below which  $\gamma$ -ray cascades are the dominant mode of de-excitation. We illustrate this situation in Fig. 3. We use  $k_\gamma = 0.5$  instead of  $k_n = 0.5$  because charged-particle emission rates can, under certain conditions, modify the position of the upper bound to the  $\gamma$ -cascade band. Thus, by " $\gamma$ -cascade band" we mean the region of excitation energy and angular momentum in a nucleus at or above the yrast levels, but below the energy at which  $k_\gamma = 0.5$ , at every angular momentum.

In the energy direction, the width of the  $\gamma$ -cascade band is about one neutron binding energy, that is, of

<sup>7</sup> More detailed calculations have been performed in which the dependences of  $k_n$  on  $\Gamma_n/D$ , on individual product levels (of neutron emission), etc., were explored using a much smaller energy mesh than was used in the present study. It was found that the region of energy over which  $\gamma$ -ray emission is comparable to neutron emission may be as large as about 2 MeV in some systems, as small as 100–200 keV in others, and depends in a detailed way on the disposition of the yrast levels (unpublished).

the order of 8 MeV, when the effect of charged-particle emission can be neglected.

### EMISSION OF $\gamma$ RAYS

We assert at this point that most of the  $\gamma$  rays are emitted from nuclei which find themselves in the  $\gamma$ -cascade band, deferring our explanation of how this comes about to the following section. Thus, whatever the calculated predictions of the  $\gamma$ -ray emission are, they are going to be particularly sensitive to what we assume about this band (e.g., the level densities in this special region, the yrast levels themselves, etc.).

Within the  $\gamma$ -cascade band we can distinguish two regions which make quite different contributions to the  $\gamma$  spectrum. The first region is above, but not on or too near the yrast line. Here the  $\gamma$ -ray emissions de-excite the nucleus, usually by a cascade of several successive dipole emissions, down onto the yrast line. This gives a "normal"  $\gamma$  spectrum, similar to those calculated by other workers who have treated the problem of cascade  $\gamma$ -ray emission.<sup>8</sup> The second region is on the yrast line itself, or very close to it. An yrast level gathers up essentially all of the population from the whole  $\gamma$ -cascade band at  $J$  values higher than its own, and can build up a very large relative cross section.<sup>9,10</sup> The yrast levels decay one to another as the population descends toward the ground state. The spectrum coming from this region does not look at all like the spectrum coming from the first region, described above. The over-all spectrum from both regions in  $\text{Dy}^{152}$  (as formed in the reaction of  $\text{Ce}^{140}$  with  $\text{O}^{16}$  at 90 MeV) is shown in Fig. 4.

Figure 4 shows the calculated spectrum of  $\gamma$  rays emitted from  $\text{Dy}^{152}$ , broken down into the contributions from dipole and quadrupole radiation. (About 70% of all the  $\gamma$  rays emitted in the reaction originate in  $\text{Dy}^{152}$ .) For  $\gamma$ -ray energies greater than 2 MeV, the calculated spectra exhibit the familiar "evaporation" shape, and it is this portion that we can associate almost entirely with the first region of the  $\gamma$ -cascade band. Below 2 MeV, there is a very sharp increase of intensity due to  $\gamma$  rays emitted in the second region.

The work of Morinaga and Gugelot,<sup>10</sup> and of Stephens, Lark, and Diamond,<sup>11</sup> shows how the great relative prominence of  $\gamma$  rays emitted in the second region can be used as an aid to their identification in favorable circumstances. In the future this should be a very important tool for studying details of nuclear de-excitation in nuclear reactions.

This clarity of the division of the  $\gamma$  spectra into two parts associated with definite regions of the  $\gamma$ -cascade

<sup>8</sup> A recent example is the work of D. Sperber, Phys. Rev. 142, 578 (1966).

<sup>9</sup> V. M. Strutinskii, Zh. Eksperim. i Teor. Fiz. 44, 1719 (1963) [English transl.: Soviet Phys.—JETP 17, 1156 (1963)]. In Eq. (15) of this paper, the right-hand side should be divided by  $\frac{1}{2}$ .

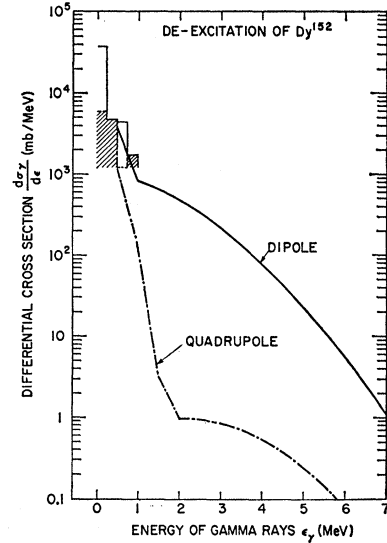
<sup>10</sup> H. Morinaga and P. C. Gugelot, Nucl. Phys. 46, 210 (1963).

<sup>11</sup> F. S. Stephens, N. L. Lark, and R. M. Diamond, Nucl. Phys. 63, 82 (1965).

band, is to some extent an artifact of the calculation. Recall that we performed our sample calculation with a fixed energy mesh of 0.5 MeV, so that we cannot display this feature very accurately. However, from the calculations described in a companion paper,<sup>3</sup> it is possible to obtain a set of values of the energy differences between adjacent yrast levels which have at least some of the irregularities and other features to be expected of yrast levels in a real nucleus. We have used these results to obtain a more complete estimate of that portion of the  $\gamma$  spectrum coming from the second region of the  $\gamma$ -cascade band, assuming that only dipole  $\gamma$ -ray emission takes place. This estimate is plotted in Fig. 4 as the solid histogram between 0 and 1.0 MeV. In making this estimate, we also corrected, approximately, for the cutoff of our calculation a few MeV above the ground state mentioned in Ref. 1. Most of the  $\gamma$  rays of lowest energy come from the region below  $J=15$ . Since practically all of the cross section reaching  $J<15$  must go through the yrast level at  $J=15$  (this is demonstrated further on), the energy of which level is taken to be 3.2 MeV, we have on the average, only 0.2 MeV per  $J$  value. This works out to be 0.2 MeV per  $\gamma$  ray if only dipole emission is assumed. It is well known, of course, that distorted even-even nuclei in this region of  $J$  and energy de-excite by cascades of quadrupole radiation, especially when in the ground-state rotational band. If all the yrast  $\gamma$  rays below  $J=15$  are quadrupole, the average energy is still only 0.4 MeV. The yrast  $\gamma$  spectrum for yrast levels above 5 MeV ( $J \geq 22$ ) is shown in Fig. 4 as a shaded histogram, to demonstrate that the softest component comes from the yrast levels of lowest spin.

We turn now to consider the special role of quadrupole  $\gamma$  radiation. Referring once again to Fig. 4, we see that by far most of the quadrupole spectrum is very soft. The hard component (above 2 MeV, say) is quite insignificant, having an intensity ratio with respect to the hard component of the dipole spectrum of the order of the input value of  $\langle \Gamma_\gamma(\text{quadrupole}) \rangle / \langle \Gamma_\gamma(\text{dipole}) \rangle$ . The bulk of the calculated quadrupole emission arises from the decay of yrast levels for which dipole emission is forbidden, but for which quadrupole emission is still possible. This can happen whenever three neighboring yrast levels are so disposed that the middle one has the highest energy. Then, at least one yrast level (not necessarily one of the three mentioned) cannot de-excite by emission of a dipole  $\gamma$  ray. If the yrast level with two units of angular momentum less (or more) than the "dipole-stranded" yrast level also has a smaller energy, quadrupole  $\gamma$ -ray emission will, in general, be the preferred mode of  $\gamma$  de-excitation of the stranded level. Only a few of these situations need occur in a given nucleus to give considerable enhancement of quadrupole  $\gamma$ -ray emission, because the cross sections for making yrast levels can be very large. The occurrence of such dipole traps for angular momenta up to and even

FIG. 4. Calculated  $\gamma$ -ray spectra arising from the de-excitation of  $\text{Dy}^{152}$  in the system  $\text{Ce}^{140} + \text{O}^{16}$  at 90 MeV (lab).



beyond  $J=40$  is a commonplace phenomenon in the shell-model calculations of yrast levels described in Ref. 3. Of course we need only cite the obvious example of the ground-state rotational band of distorted even-even nuclei for evidence that such dipole traps in yrast levels are well known experimentally.

It should be noted at this point that the calculation gives a very natural explanation for enhancement of quadrupole  $\gamma$ -ray emission, one which does not really require special assumptions about the collective nature of nuclear levels. The arguments for collective behavior of levels of very high angular momentum might therefore have to be made on grounds other than only enhancement of quadrupole emission relative to dipole emission.

It is of interest to estimate how large the proportion of quadrupole  $\gamma$  radiation can reasonably be expected to be in a calculation such as this one. An upper limit to the amount of energy carried away by  $\gamma$  cascades, mainly of dipole radiation, in the first region (defined above) of the  $\gamma$ -cascade band, is just the width of this band. It is more reasonable to expect the actual value to be nearer half this, and 6 MeV might be a realistic rule-of-thumb figure to work with in the example we have been discussing. Thus for  $\text{Dy}^{152}$ , in which 15 MeV (see Table I of Ref. 1) of total energy was carried away by  $\gamma$  radiation, we have that about 9 MeV was carried away by yrast-level-to-yrast-level transitions characteristic of the second region of the  $\gamma$ -cascade band. Now if every second yrast level happens to be a dipole trap, as is the case in the ground-state rotational band of many distorted even-even nuclei, then essentially this entire 9-MeV total energy of second-region  $\gamma$  radiation must appear as quadrupole radiation. We can see from Fig. 4 that the average  $\gamma$ -ray energy in the first region is about 2 MeV, while doubling the mean energy of the solid histogram gives an average  $\gamma$ -ray energy from the

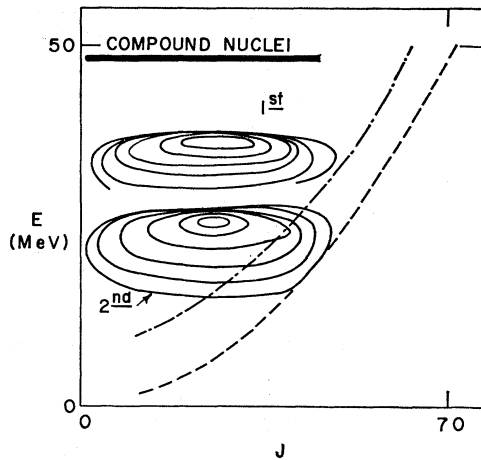


FIG. 5. Schematic diagram illustrating the successive regions of energy and angular momentum most heavily populated by neutron emission during the de-excitation of an ensemble of highly excited compound nuclei of a given species (e.g.,  $Dy^{156}$ ). The distribution of angular momentum is roughly to scale for a 100-MeV heavy-ion bombardment of a medium-heavy target.

second region, if it is taken to be quadrupole radiation only, of about 0.5 MeV. Together with the above total-energy estimates, these average energies allow us to conclude that as many as 85% of the  $\gamma$ -ray photons could, under the above-described special circumstances, be emitted as quadrupole radiation. Mollenauer's conclusion<sup>12</sup> that in some of the cases he studied essentially all of the  $\gamma$  radiation is emitted by quadrupole transitions, is thus not at all contradicted by our calculation.

If, as suggested in Ref. 3, it should happen that the matrix elements for transitions from yrast level to yrast level are, on the average, much smaller than transitions to levels just above the yrast levels, then the above picture would have to be suitably modified.

### THE DISTRIBUTION OF POPULATION

Since our sample calculation is restricted to the compound-nucleus model, we are concerned with the de-excitation of an assembly of  $Dy^{156}$  nuclei, all excited to the same high energy. They are distributed over a very wide range of angular momenta, however. The emission of a neutron from each  $Dy^{156}$  nucleus then gives  $Dy^{155}$  distributed over both angular momentum and energy, the energy distribution reflecting the shape of the spectrum of emitted neutrons. The emission of a second neutron similarly yields  $Dy^{154}$  nuclei distributed over both angular momentum and energy, but the spread of energies over which most of the  $Dy^{154}$  nuclei are to be found is broader than it was for  $Dy^{155}$ . Subsequent neutron emissions may broaden the energy distributions still more, of course. The features just described are illustrated schematically in Fig. 5.

Now the maximum energy of the  $Dy^{155}$  population dis-

tribution is less than the energy of the  $Dy^{156}$  compound nuclei by just the binding energy of a neutron in  $Dy^{156}$ . Likewise the maximum energy for any given population distribution is less than the energy of the  $Dy^{156}$  compound nuclei by the binding energy of the requisite number of neutrons which must be emitted to form the nucleus in question. The most probable energy for each successive population distribution is thus decreased by somewhat more than a neutron binding energy with each successive neutron evaporation. On the other hand, the distribution of population with respect to angular momentum changes but little in the successive neutron evaporations, with an important exception described further on.

The successive emission of neutrons continues as described above, until an appreciable part of the population distribution falls within the  $\gamma$ -cascade band. Such a situation is illustrated by the lower contour diagram in Fig. 5. Most of the population falling in the  $\gamma$ -cascade band ultimately reaches the ground state via cascades of  $\gamma$ -ray emissions, while most of the population falling above the  $\gamma$ -cascade band proceeds to emit another neutron.

Population distributions in our sample calculation are shown in Figs. 6(a)–6(c); Fig. 6(b) is the population distribution in  $Dy^{152}$  given by neutron emission from  $Dy^{153}$ , before the calculation of the de-excitation of  $Dy^{152}$  contour represents the locus of constant relative population (given here in mb per 0.5 MeV per unit of spin), and differs from its neighboring contour by a factor  $\sqrt{10}$ . The point  $\otimes$  represents the peak of the distribution. Figure 6(c) shows the "population" distribution in  $Dy^{152}$  after the calculation of its de-excitation was completed [ $P_5(EJ)$  in the notation of Ref. 1]. The distribution that the contours now represent is the integrated total population experienced by the nucleus at every excitation energy and angular momentum. Each point represents the sum of the population contributed by neutron emission [i.e., the distribution in Fig. 6(b)] plus all the contributions from  $\gamma$ -ray de-excitations of  $Dy^{152}$  nuclei at higher energies; Fig. 6(a) is the same as Fig. 6(c) except that it is drawn for  $Dy^{153}$ . In both Figs. 6(a) and 6(c) we see clearly the consequences of the steep rise in  $k_\gamma$  with decreasing energy, for energies less than those for which  $k_\gamma=0.5$ . In addition, we indicate the cross sections (in mb) for formation of a few of the yrast levels themselves. Yrast levels with angular momenta as large as  $40\hbar$  may be formed with very large cross sections of order 40 mb or more, toward the end of the neutron evaporation chain (e.g., in  $Dy^{152}$ ). We take up this point again further on.

It is quite clear from Figs. 6(a)–6(c) that most of the  $\gamma$  rays arising in these reactions are generated within the  $\gamma$ -cascade band after the last neutron-evaporation step. Also, it is clear that the properties of the  $\gamma$ -cascade band just above the yrast levels (excluding the

<sup>12</sup> J. F. Mollenauer, Phys. Rev. **127**, 867 (1962).

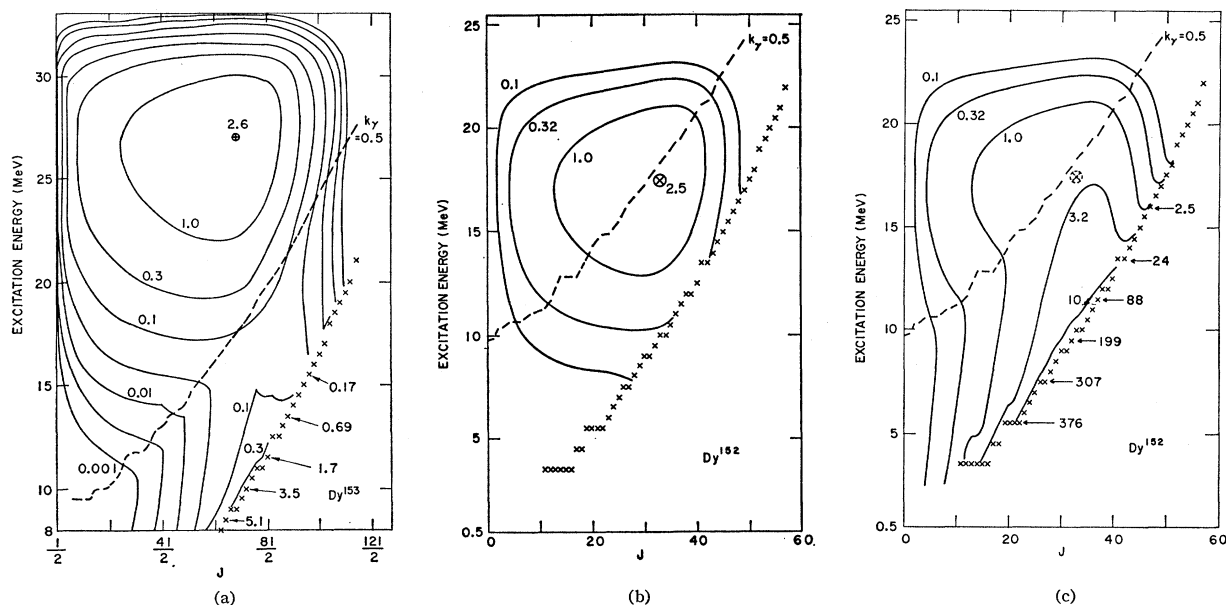


FIG. 6. Calculated "population distributions" in  $Dy^{152}$  and  $Dy^{153}$  appearing during sample calculations of  $Ce^{140}+O^{16}$  at 90 MeV (see text). (a) Population distribution in  $Dy^{153}$  including buildup due to  $\gamma$ -ray de-excitation cascade. (b) Population distribution in  $Dy^{152}$  arising from neutron emission from  $Dy^{153}$ , but before  $\gamma$ -ray de-excitation was calculated. (c) Population distribution in  $Dy^{152}$  after de-excitation has been calculated. The contours in (a) and (c) represent the largest population ever experienced at each point  $E, J$ .

yrast levels themselves, for a moment) have a disproportionate influence on the over-all  $\gamma$ -ray spectrum, because the population is highest there. Thus, the level densities used in calculations such as this one must accurately reflect the properties of the nuclear levels just above the yrast levels, if the  $\gamma$ -ray spectrum is to be reasonably well reproduced. This is the reason we went to such pains to be able to introduce the "yrast temperature"  $T_J$  explicitly into our calculations.<sup>13,14</sup> The large contribution from the  $\gamma$ -cascade band, and the correspondingly enhanced effect of the low "nuclear temperatures" in the  $\gamma$ -cascade band, are displayed in Fig. 7. Here, we show the  $\gamma$ -ray spectra arising from dipole emission from  $Dy^{156}$  through  $Dy^{152}$ . The amount of population falling in the  $\gamma$ -cascade bands of  $Dy^{156}$ ,  $Dy^{155}$  and  $Dy^{154}$  is negligible, and the  $\gamma$  spectra thus take the simple "evaporation" form [see Eq. (12) of Ref. 1]. The slowly decreasing high-energy portion of each of these spectra reveals the high nuclear temperature prevailing near the excitation energies at which they are emitted. It should also be noticed that most of these  $\gamma$ -ray emissions are followed by particle emission. The first really appreciable population of the  $\gamma$ -cascade band appears for  $Dy^{153}$  in this case. The difference between the  $\gamma$ -ray spectra for  $Dy^{154}$  and  $Dy^{153}$  is quite striking. Not only does the  $\gamma$ -ray spectrum from  $Dy^{153}$  decrease much more rapidly with increasing

energy than does the spectrum from  $Dy^{154}$ , but it is two orders of magnitude more intense. The spectra from  $Dy^{152}$  and  $Dy^{151}$  (not plotted) carry this trend much further.

A comparison of Fig. 4 of Ref. 2 with Figs. 6(a) to 6(c) reveals that appreciable population falls into the region where  $k_\alpha$  (i.e., the fraction of nuclei emitting

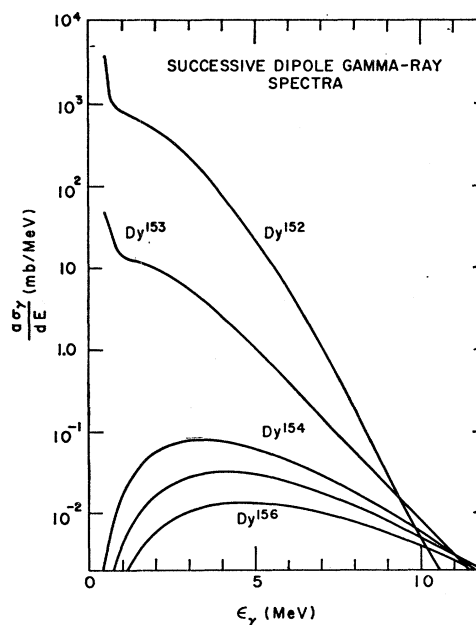


Fig. 7. Calculated dipole  $\gamma$ -ray spectra from several Dy isotopes in the cascade de-excitation of  $Dy^{156*}$ .

<sup>13</sup> The problem of the rate of decrease with increasing energy of the level spacings just above the yrast levels has been neglected until recently. The only treatments of this problem of which we are aware are those of D. W. Lang (Ref. 14) and of Grover (Ref. 3).

<sup>14</sup> D. W. Lang, Nucl. Phys. **77**, 545 (1966).

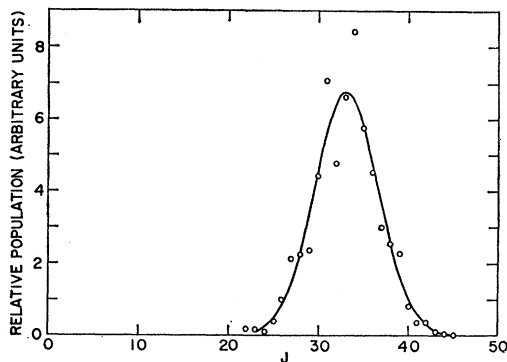


FIG. 8. "Independent yields" (see text) of yrast levels in  $Dy^{152}$  calculated for the de-excitation of  $Dy^{156*}$  at  $J=40$  and  $E=58.5$  MeV.

alpha particles) displays maxima for  $Dy^{152}$  and  $Dy^{151}$ . Also, comparison of Figs. 4 and 5 of Ref. 2 with the cross sections for forming yrast levels, given in Figs. 6(a) and 6(c), shows that there is a large cross section for forming those yrast levels for which dipole emission cannot take place, and for which  $k_\alpha$  is consequently especially large compared to  $k_\alpha$  for the other yrast levels. The appearance of the type-II and type-III alpha-particle subspectra<sup>2</sup> thus depends on the population falling in the  $\gamma$ -cascade band. Referring to Fig. 6 of Ref. 2 we see that  $Dy^{156}$ ,  $Dy^{155}$ , and  $Dy^{154}$  display essentially only type-I alpha-particle subspectra, just as they display only normal "evaporation"  $\gamma$ -ray spectra (Fig. 7). Beginning with  $Dy^{153}$  we see the admixture of type-II and type-III subspectra, in addition to the type-I subspectrum. In  $Dy^{152}$  and  $Dy^{151}$  the type-II and type-III subspectra are dominant. All this is necessarily, of course, parallel with the behavior of the  $\gamma$ -ray spectra. Notice especially that the type-II and type-III alpha-particle subspectra appear *together*; this suggests another experimental test.

Before tracing the dissipation of angular momentum in our example system, it is helpful to gain additional insight into the de-excitation process by a study of the calculated decay properties of a compound nucleus having not only a unique excitation energy, but also a unique angular momentum. We describe some of our results for the calculated de-excitation of a nucleus having an excitation energy of 58.5 MeV (this is the same excitation energy as results from the amalgamation of an  $O^{16}$  projectile with a  $Ce^{140}$  target nucleus, at a laboratory energy of 90 MeV) and an angular momentum of  $40 \hbar$ . The mean angular momentum of the states populated in  $Dy^{155}$  by neutron emission, but before calculation of the de-excitation of the  $Dy^{155}$ , is  $38.8 \hbar$ . The mean angular momentum of all the states populated in the  $\gamma$ -cascade band of  $Dy^{152}$  by neutron emission from  $Dy^{153}$ , before calculating the de-excitation of  $Dy^{152}$ , is  $35.0 \hbar$ . Thus, the successive emission of four neutrons has resulted in the removal of about 5.0 units of angular momentum, on the average, from the original system;

this is about 1.25 units per neutron emission. Thomas<sup>15</sup> and others<sup>16,17</sup> likewise have calculated that the amount of angular momentum removed by neutron emission should be of order  $1 \hbar$ , in systems roughly similar to the one we consider. Recall that we have distinguished two qualitatively different stages through which a nucleus de-excites itself to the ground state by  $\gamma$ -ray emission: (1) A "normal" cascade of  $\gamma$ -ray emissions, mainly dipole, takes place, ultimately terminating at an yrast level; (2) the yrast level then decays, mostly through a sequence of yrast levels, one into another, until the ground state is reached. We are interested in knowing how much angular momentum is dissipated in each mode. In Fig. 8 we display the relative population of yrast levels in  $Dy^{152}$  which comes only from the decay of nonyrast levels (i. e., the "independent yields," where the contribution from other yrast levels has been subtracted). The mean angular momentum of this distribution is  $33.1 \hbar$ . The smooth curve drawn through the points is a Gaussian one, with a full width at half-maximum of  $8.3 \hbar$ . The scatter in the points reflects the unsmoothness of the yrast levels used as input to the calculation.<sup>18</sup> Thus, the  $\gamma$ -ray cascade of stage (1) above has removed 1.9 units of angular momentum, and the remaining  $33.1$  units is dissipated in the cascade of  $\gamma$ -ray emissions of stage (2).

Returning to our more realistic example calculation for  $Ce^{140}+O^{16}$ , we have plotted in Fig. 9 the "independent yields" of yrast levels for the four products formed with the greatest yield. The mean angular momenta which must be dissipated by  $\gamma$ -cascades of mode (2), for  $Dy^{151}$  and  $Dy^{152}$ , are  $19.5 \hbar$  and  $30.3 \hbar$ , respectively, and the corresponding average per reaction is about  $24.8 \hbar$ . This is to be compared with an average angular momentum for the initial compound nuclei of  $30.1 \hbar$ . Since an average of 4.50 neutrons was emitted, the average angular momentum carried away "per nucleon" is about  $1.2 \hbar$ ; of course this figure also includes the angular momentum carried away by the cascade of  $\gamma$ -ray emission in stage (1).

Referring to the data analysis of Alexander and Simonoff,<sup>19</sup> we see at once that their estimate, of 2 to 4 units of angular momentum removed by the first neutron may be too large. Even though we are able to duplicate their data rather well, we calculate that an average of only 0.85 units of angular momentum is dissipated by emission of the first neutron. However, a systematic analysis of excitation functions and other data for several of the systems they investigated is

<sup>15</sup> T. D. Thomas, Nucl. Phys. **53**, 577 (1964).

<sup>16</sup> D. G. Sarantites and B. D. Pate, Nucl. Phys. **A93**, 545 (1967).

<sup>17</sup> G. A. Pik-Pichak, Zh. Eksperim. i Teor. Fiz. **38**, 768 (1960) [English transl: Soviet Phys.—JETP **11**, 557 (1960)].

<sup>18</sup> This effect is itself an important phenomenon, with obvious consequences for the interpretation of isomer-ratio measurements (unpublished).

<sup>19</sup> J. M. Alexander and G. N. Simonoff, Phys. Rev. **133**, B93 (1964).

required before an adequate evaluation of the usefulness of their approximate analysis can be made.

Although we do not report calculated excitation functions in this paper, some major features to be expected of excitation functions can be inferred from Figs. 5, 6, and 9. Near threshold for forming a nuclide (as with  $\text{Dy}^{150}$  in our example), only the levels of lowest angular momentum are populated. The levels of higher angular momentum are not populated because their corresponding yrast levels have a threshold energy which exceeds the bombarding energy. As the bombarding energy rises, it becomes possible to form levels of larger and larger angular momentum. When the threshold for emitting an additional neutron is exceeded, the additional neutron emission will preferentially de-excite the nuclei of lowest angular momentum, and we arrive at a situation like that shown for  $\text{Dy}^{152}$  [Figs. 6(b), 6(c), and 9]. The excited nuclei of smaller angular momenta tend ultimately to form the less massive products, and those of larger angular momenta the heavier products, although the discrimination is far from being a sharp one. (When this phenomenon is reflected in isomer-ratio measurements, it is sometimes called<sup>20-22</sup> "spin fractionation.") Finally, for some nuclear species the highest angular momenta brought in by the incident particle may be exceeded by the yrast levels, at energies in the range encompassing most of the excited levels populated by neutron emission, in the given nuclear species. Then this nuclear species, and those involving the emission of even fewer nucleons, will be made with only small cross sections; this is the situation for  $\text{Dy}^{153}$ , shown in Figs. 6(a) and 9. Thus, as the bombarding energy rises, and the mode of formation of a given product changes in the way outlined above, we can see why the average energy and angular momentum removed by  $\gamma$ -ray emission in forming this same product rises steadily.

Alexander and Simonoff,<sup>23</sup> Seegmiller,<sup>24</sup> and Kiefer<sup>25</sup> noticed that successful semiquantitative predictions of isomer ratios in nuclear reactions can often be made using a very crude model in which it is assumed that of the compound nuclei leading to the product, those having less than some critical spin lead always to the low-spin isomer, while those having larger spins lead to the high-spin isomer. The critical spin is experimentally determined near the peak of the excitation function. In terms of the foregoing discussion it is easy to see why such a simple approach works as well as it does, and where and how it becomes unreliable. As we

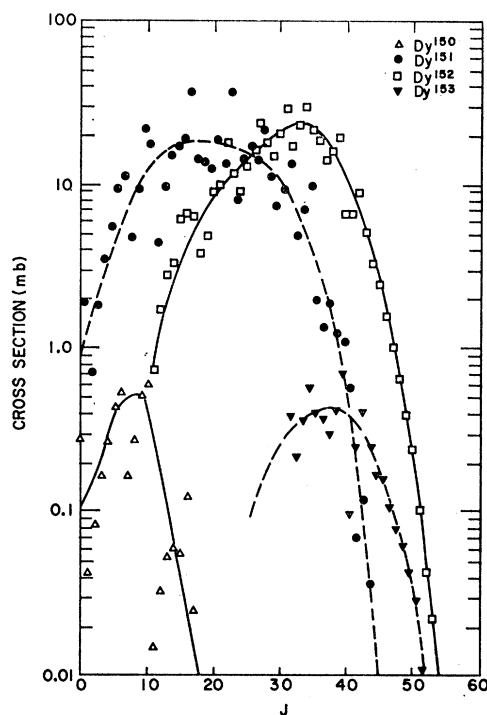


FIG. 9. "Independent yields" of yrast levels in  $\text{Dy}^{150}$ ,  $\text{Dy}^{151}$ ,  $\text{Dy}^{152}$ , and  $\text{Dy}^{153}$  in the realistic sample calculation for the system  $\text{Ce}^{140} + \text{O}^{16}$  at 90 MeV (lab). The smooth curves are only to aid in picking out the points belonging to a particular nuclear species.

have described, for compound nuclei initially having large angular momenta, most of the angular momentum is removed by the yrast cascades. A cascade proceeding along the yrast levels at spins greater than that of the high-spin isomer will almost surely end at the high-spin member. Thus, almost all the compound nuclei having more than a certain spin (within reasonably narrow limits, e.g., see Fig. 8) will lead to the high-spin isomer. The small amount of angular momentum taken up by the neutrons, and by the photons in the first stage of  $\gamma$ -ray emission often serves to raise the effective critical spin to somewhat larger values than the nominal one midway between the spins of the two isomers. We see from Fig. 9 that for our calculated example the simple rule would predict too much high-spin isomer for  $\text{Dy}^{151}$ , and too little for  $\text{Dy}^{152}$  (assuming for the sake of argument that  $\text{Dy}^{151}$  and  $\text{Dy}^{152}$  have isomeric states). However, for energies not too far from the excitation function maximum it would not be too inaccurate, because the "independent-yield" distributions are quite broad. It would predict somewhat too much high-spin isomer at smaller energies and too little at larger energies. At very small energies, where but little angular momentum is given to the compound nuclei on the average, the angular momenta contributed by neutron and stage-one photon emission would become important (see Fig. 8), and the rule would again predict too little of the high-spin isomer. This pattern is

<sup>20</sup> C. Riley and B. Linder, Phys. Rev. **134**, B559 (1964).

<sup>21</sup> C. T. Bishop, J. R. Huizenga, and J. P. Hummel, Phys. Rev. **135**, B401 (1964).

<sup>22</sup> N. D. Dudey, and T. T. Sugihara, Phys. Rev. **139**, B896 (1965).

<sup>23</sup> J. M. Alexander and G. N. Simonoff, Phys. Rev. **130**, 2383 (1963).

<sup>24</sup> D. W. Seegmiller, University of California Radiation Laboratory Report No. UCRL 10850, 1963 (unpublished).

<sup>25</sup> R. L. Kiefer, University of California Radiation Laboratory Report No. UCRL 11049, 1963 (unpublished).



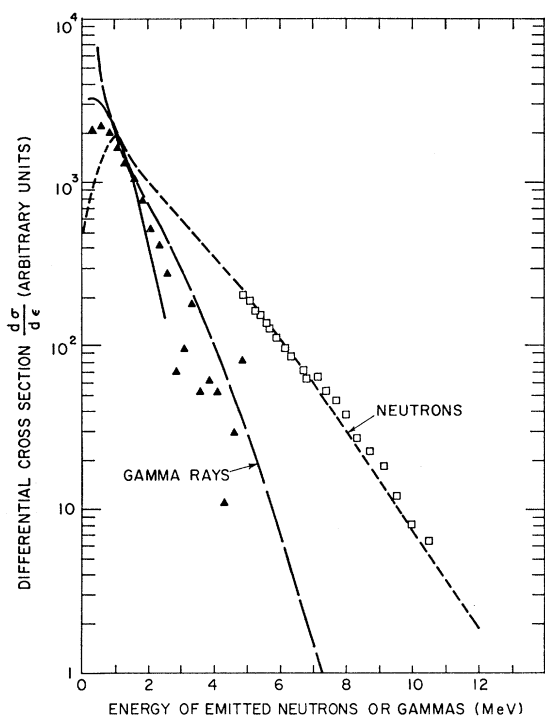


FIG. 10. Comparison of some experimental  $\gamma$ -ray and neutron spectra for heavy-ion reactions with medium-heavy targets, with calculations done in this study. The solid line is the  $\gamma$  spectrum measured by Oganesyan *et al.* (Ref. 27) for the system  $\text{Ta}^{181} + \text{O}^{16}$  at 100 MeV, and the closed triangles represent the  $\gamma$  spectrum measured by Mollenauer (Ref. 12) for the system  $\text{Ho}^{165} + \text{C}^{12}$  at about 110 MeV. The open squares represent the neutron spectrum measured by Kumpf *et al.* (Ref. 28) for the system  $\text{Ar}^{40} + \text{Sn}$  at 0–170 MeV (thick target). The dashed lines give the calculated spectra for the system  $\text{Ce}^{140} + \text{O}^{16}$  at 90 MeV.

indeed just what is observed in comparison with experiment.<sup>24</sup>

### EXPERIMENTAL VERIFICATION

Although there exists a sizable body of excitation-function and recoil data with which models of nuclear evaporation can be tested (e.g., Ref. 19) it already seems possible that it will present no insuperable inconsistencies. Certainly the “first-try” success described in the first paper<sup>1</sup> of this series implies as much; however, it is still reasonable to expect that more complete analyses will reveal inadequacies in the model, especially for the targets of smaller mass (see especially Ref. 26). Unfortunately, such data as those of Ref. 19 do not really test many detailed consequences of the model, such as the pattern of  $\gamma$ -ray de-excitation and the flow of population in excited states that we have described.

More stringent tests can be made with spectra of particles and photons, but no data of this kind exist for our sample system, and few exist at all for any system for cases in which the bulk of the reaction may

<sup>26</sup> M. Kaplan and A. Ewart, *Phys. Rev.* **148**, 1123 (1966).

be expected to proceed through a compound nucleus without fissioning. It is still instructive, however, to compare with our calculated spectra the experimental photon and neutron spectra taken in heavy-ion bombardments of medium-heavy targets. This is done in Fig. 10. The experimental  $\gamma$ -ray spectra are for the systems  $\text{Ho}^{165} + \text{C}^{12}$  (about 110 MeV, 45°, lab)<sup>12</sup> and  $\text{Ta}^{181} + \text{O}^{16}$  (100 MeV, 115°, lab).<sup>27</sup> The experimental neutron spectrum is for the system  $\text{Ar}^{40} + \text{Sn}$  (170 MeV, 145°, thick target, lab).<sup>28</sup> All the experimental data are arbitrarily normalized to our calculation (at 1.5 MeV for the  $\gamma$ -ray spectra, and at 7 MeV for the neutron spectrum).

In all cases, the energy trend of the experimental data is reasonably well duplicated in our calculation. That the  $\gamma$ -ray spectra decrease more steeply with increasing energy than the neutron spectrum suggests that the level densities and distributions in the  $\gamma$ -cascade band i.e., the “yrast temperatures” and yrast levels) are at least qualitatively similar to those we have assumed in our calculation. This is consistent with, but does not test very well, the specific pattern that our assumed model gives, namely that most of the angular momentum is carried away by yrast-level-to-yrast-level transitions. Remember, however, that the experimental spectra are for rather different systems, so definite conclusions cannot be drawn.

To some extent, whether there is a large contribution of yrast-level-to-yrast-level transitions might be tested by experiments designed to verify the energy dependence of the quadrupole/dipole ratio displayed in Fig. 4. It may be possible to show, by angular distributions, or by delayed-coincidence measurements, that the low-energy  $\gamma$ -ray photons ( $\leq 1$  MeV) arise to a much larger extent by quadrupole transitions than do the higher-energy photons ( $\geq 2$  MeV), for  $\gamma$ -ray energies not too high.

Another experiment that has been suggested to test the same point is to measure the independent yields of yrast levels in cases where they can be identified. Indeed, in certain circumstances, it may prove possible to do this.<sup>29,30</sup>

Whether the neutrons carry off as little angular momentum as they are calculated to do seems a difficult point to check. In our calculation they could carry off  $3\hbar$  on the average, instead of  $1\hbar$ , and the effect on the final results would be difficult to see. Probably, the competition between neutron emission and the emission of heavier fragments, such as alpha particles, would be more sensitive to this feature than are excitation functions and neutron and photon spectra.

<sup>27</sup> Yu. Ts. Oganesyan, Yu. V. Lobanov, B. N. Markov, and G. N. Flerov, *Zh. Eksperim. i Teor. Fiz.* **44**, 1171 (1963) [English transl.: *Soviet Phys.—JETP* **17**, 791 (1963)].

<sup>28</sup> H. Kumpf, L. Kumpf, and Shih Shuang-hui, *Yadernaya Fiz.* **1**, 264 (1965) [English transl.: *Soviet J. Nucl. Phys.* **1**, 186 (1965)].

<sup>29</sup> I. Halpern (private communication).

<sup>30</sup> R. M. Diamond (private communication).

Certainly, there is much work to be done, but now that it is known to be feasible to analyze these complex systems with the help of computers, we need not hesitate to undertake the necessary experiments.

#### ACKNOWLEDGMENTS

We are indebted to Dr. R. M. Diamond, Professor I. Halpern, and Professor H. Morinaga for helpful discussions.

PHYSICAL REVIEW

VOLUME 157, NUMBER 4

20 MAY 1967

## Emission of Alpha Particles from Nuclei Having Large Angular Momenta\*

J. ROBB GROVER

*Chemistry Department, Brookhaven National Laboratory, Upton, New York*

AND

JACOB GILAT†

*Chemistry Department, State University of New York at Stony Brook, Stony Brook, New York and  
Chemistry Department, Brookhaven National Laboratory, Upton, New York*

(Received 29 July 1966)

The statistical theory of nuclear de-excitation predicts  $\alpha$ -particle energy spectra having important features that were missed in earlier, less complete calculations. To a good approximation, the  $\alpha$  spectrum is composed of three qualitatively different subspectra. For  $\text{Dy}^{156*}$  compound nuclei formed by  $\text{Ce}^{140} + \text{O}^{16}$  at 90 MeV (lab), these subspectra have their respective maxima at 17, 12, and 7.5 MeV. The 7.5-MeV subspectrum should be resolvable into a group of sharp lines. The crucial roles of the lowest excited state at every angular momentum (the yrast levels), and of the competition with neutron and with dipole and quadrupole  $\gamma$ -ray emission, are stressed. Simple formulas are derived for estimating the energies at the maxima of the two lowest-energy subspectra. Since the  $\alpha$ -particle subspectra are predictions of the most widely used version of the statistical model of nuclear de-excitation, a failure to observe them would be important. If they are observed, the experimental data should provide information about several nuclear properties heretofore inaccessible.

### INTRODUCTION

**N**UCLEAR reactions in which  $\alpha$  particles are emitted with unexpectedly large probability at energies well below the Coulomb barrier have been observed.<sup>1-7</sup> Explanations for this phenomenon have

included suggestions that the emitting nuclei are non-spherical,<sup>2,5,8,9</sup> that the Coulomb barrier decreases with increasing excitation energy,<sup>6,10</sup> that the Coulomb barrier may be perturbed by intense localized heating over a small volume of the nucleus,<sup>7</sup> that localized heating may cause a local expansion of nuclear matter to a large radius before particle emission,<sup>11</sup> that alphas may be emitted to an important extent from the products of high-energy fission,<sup>7</sup> and that such alphas are emitted from nuclei excited to energies less than nucleon binding energies, but greater than alpha binding energies.<sup>12</sup> In carrying through the calculations for the statistical theory of nuclear de-excitation more completely than has been done previously, we find that sub-barrier  $\alpha$  particles are predicted without making special assumptions about nuclear shapes, etc. (see Fig. 6), partly by the simple process described in the last of the explanations cited above, but much more importantly, when the same nuclei possess large angular momenta, in related processes in which the  $\alpha$  particles

\* Research performed in part under the auspices of the U. S. Atomic Energy Commission.

† Present address: Israel Atomic Energy Commission, Soreq Nuclear Research Center, Yavne, Israel.

<sup>1</sup> M. Lefort, J. P. Cohen, H. Dubost, and X. Tarrago, *Phys. Rev.* **139**, B1500 (1965).

<sup>2</sup> H. Dubost, M. Lefort, J. Peter, and X. Tarrago, *Phys. Rev.* **136**, B1618 (1964).

<sup>3</sup> J. Muto, H. Itoh, K. Okano, N. Shiomi, K. Fukuda, Y. Omori, and M. Kihara, *Nucl. Phys.* **47**, 19 (1963).

<sup>4</sup> H. C. Britt and A. R. Quinton, *Phys. Rev.* **124**, 877 (1961).

<sup>5</sup> W. J. Knox, A. R. Quinton, and C. E. Anderson, *Phys. Rev.* **120**, 2120 (1960).

<sup>6</sup> C. B. Fulmer and C. D. Goodman, *Phys. Rev.* **117**, 1339 (1960).

<sup>7</sup> J. B. Harding, S. Lattimore, and D. H. Perkins, *Proc. Roy. Soc. (London)* **A196**, 325 (1949). See also Refs. 16 and 17 for additional references to relevant work done at about this time. This paper on cosmic-ray stars in emulsion is cited because the data it reports inspired ideas about how sub-barrier  $\alpha$ -particle emission might be explained. On the basis of more recent measurements, however, the "sub-barrier"  $\alpha$ 's seen in GeV proton irradiations of AgBr emulsions are convincingly explained as merely  $\alpha$ 's that are evaporated in the backward direction from recoiling excited nuclei. See E. W. Baker, S. Katcoff, and C. P. Baker, *Phys. Rev.* **117**, 1352 (1960); N. T. Porile, *Phys. Rev.* **135**, B371 (1964).

<sup>8</sup> R. Beringer and W. J. Knox, *Phys. Rev.* **121**, 1195 (1961).

<sup>9</sup> D. V. Reames, *Phys. Rev.* **137**, B332 (1965).

<sup>10</sup> E. Bagge, *Ann. Physik.* **33**, 389 (1938).

<sup>11</sup> T. Miyazima, K. Nakamura, and Y. Futami, *Progr. Theoret. Phys. (Kyoto)*, Suppl. 621 (1965).

<sup>12</sup> D. W. Lang, *Phys. Rev.* **123**, 265 (1961).